

Fluorination of Vulcan XC-72R for cathodic microporous layer of passive micro direct methanol fuel cell

Mei Chen · Shengjun Wang · Zhiqing Zou ·
Ting Yuan · Zhilin Li · Daniel L. Akins ·
Hui Yang

Received: 21 January 2010 / Accepted: 5 September 2010 / Published online: 16 September 2010
© Springer Science+Business Media B.V. 2010

Abstract The effect of adding fluorinated Vulcan XC-72R into the microporous layer (MPL) of the cathode in a passive micro direct methanol fuel cell (μ DMFC) has been investigated. Upon fluorination with fluoro-alkyl silane (FAS), the surface of XC-72R becomes more hydrophobic, as indicated by contact angle measurements. The performance of the membrane electrode assembly (MEA) is improved significantly when fluorinated Vulcan XC-72R is used in MPL of the cathode. The maximum power density of a passive μ DMFC reached ca. 36.2 mW cm^{-2} at room temperature, and the constant-current discharging test exhibits enhanced stability. Also observed is a decreased water transport coefficient (α), calculated from discharging test, attributable to the greater hydrophobicity resulting in higher liquid pressure on the cathode, which forces more water to flow back to the anode. Additionally, A.C. impedance analysis indicates that the improvement in performance results from the decrease of charge transfer resistance of the cathodic reaction.

Keywords Fluorination · Cathodic microporous layer · Membrane electrode assembly · Passive micro direct methanol fuel cell · Electrochemical impedance

M. Chen · S. Wang · Z. Zou · T. Yuan · Z. Li · H. Yang (✉)
Energy Science and Technology Laboratory, Shanghai Institute of Microsystems and Information Technology,
Chinese Academy of Sciences, Shanghai 200050, China
e-mail: hyang@mail.sim.ac.cn; huiyang65@hotmail.com

M. Chen · S. Wang
Graduate School of the Chinese Academy of Sciences,
Beijing 100039, China

D. L. Akins
CASI and Department of Chemistry, The City College
of the City University of New York, New York, NY 10031, USA

1 Introduction

The direct methanol fuel cell is regarded as a potential power source for portable electronic devices such as notebook computers, personal digital assistants (PDAs), and mobile telephones due to its high energy conversion efficiency, simple structure, convenient delivery and storage of liquid fuel, and operation at normal ambient conditions [1, 2]. The passive micro direct methanol fuel cell (μ DMFC), especially, is the most attractive because of its simplicity [3, 4]. In a passive μ DMFC system, fuel and oxidant are supplied to the electrodes by natural diffusion, which decreases the volume of the fuel cell system, substantially reduces weight and parasitic power, increases the achievable energy density and power density, and reduces the cost of the fuel cell system. However, several challenges must be addressed before practical application, which include cathodic water flooding, slow oxygen mass transfer, and severe methanol crossover [5–7].

Water management significantly affects the performance and durability of DMFCs. For a passive μ DMFC (under air-breathing mode), the oxygen reduction reaction rate at the cathode depends on the transport rate of oxygen from the flow channels to the catalytic active sites, which occurs through natural diffusion. Under atmospheric pressure, significant importance is attached to the management of water and gas employed by the gas diffusion layer (GDL) in the cathode of a passive μ DMFC [2, 8, 9]. The cathodic GDL, usually composed of a backing layer (BL; carbon fiber paper or carbon cloth) and a microporous layer (MPL), serves as the pathway for the diffusion of air into the cathode and a conduit for the removal of the byproduct water from the cathode. The MPL, placed between the catalyst layer and BL, plays an important role for improving both the cell performance and stability [10–13].

It minimizes electric contact resistance between the catalyst layer and the macroporous carbon substrate by forming a flat and uniform layer, and also prevents the catalyst from leaking into the BL, thereby increasing the catalyst utilization and reducing the tendency of electrode flooding. Extensive experimental work has been done by numerous researchers regarding the effects of the type and loading level of carbon powders, the effect on the content of polytetrafluoroethylene (PTFE), as well as the effect on cell performance of adding pore-forming agents in the MPL [14–18]. Much work has focused on the impact of hydrophilic/hydrophobic character and porosity in the cathodic MPL on water transport through the membrane. Specifically, Lu et al. [19] reported that a highly hydrophobic cathodic MPL built up the hydraulic pressure at the cathode which drove the water from the cathode into the anode and restrained the flow of water associated with electro-osmosis. Xu et al. [20] investigated the effects of both the PTFE and carbon loadings within cathodic MPLs. It was found that the PTFE loading in the MPL had a substantial effect on cell performance. Increased PTFE loading revealed two effects: increased hydrophobic level and decreased porosity of the MPL as the PTFE film formed. Additionally, experimental results showed that increase in the carbon loading in the MPL significantly lowered the water-crossover flux. An MPL consisting of 40 wt% PTFE with a 2.0 mg cm⁻² carbon loading was found to exhibit the best cell performance and lowest water-crossover rate. Krishnamurthy et al. [21] also claimed that the PTFE content in the MPL affects the performance of a DMFC. Specifically, PTFE content is found to affect the catalyst utilization and cell impedance values. From previous reports, it is noted that the hydrophobic property in the MPL significantly affects DMFC performance. Improvement of hydrophobicity not only increases the hydraulic pressure that drives water backwards, but also accelerates gas transfer. Earlier works have focused on improving MPL hydrophobicity by increasing PTFE content within the MPL. However, PTFE aggregates easily and forms a film that lowers the porosity of the MPL. In the present work, carbon powder, Vulcan XC-72R, is modified with fluoro-alkyl silane (FAS), which will lead to a decrease in surface free energy, and increases the hydrophobicity of the cathodic MPL, while, also, avoiding blockage to the flow of both gas and water.

2 Experimental

2.1 Fluorination of Vulcan XC-72R and characterization

A commercial Vulcan XC-72R (Cabot) carbon black was oxidized with 8 M nitric acid at 80 °C and refluxed for

24 h. After the acid treatment, the mixture was filtered, washed until the filtrate reached neutral pH, and dried overnight at 100 °C. The oxidized carbon was labeled XC-72R-HNO₃. The nitric acid treated XC-72R was then fluorinated by dodecafluoroheptyl-propyl-trimethoxysilane (C₁₃F₁₂H₁₈SiO₃; Xeogia Fluorine Silicon Chemical Co.) 20 vol% in ethanol solvent at 50 °C, and refluxed for 2 days. The fluorinated carbon was filtered and dried overnight at 70 °C under vacuum (labeled as F-XC-72R).

The samples were then characterized by FT-IR spectroscopy. IR measurements of XC-72R, XC-72R-HNO₃, and F-XC-72R were conducted using KBr pellet method.

The hydrophobic character of carbon materials was investigated using a contact angle measuring system, DSA100. The carbon materials (XC-72R, XC-72R-HNO₃, F-XC-72R) and PTFE (weight ratio 4:1) were mixed and spread onto carbon cloth (Type A, 20 wt% PTFE, E-TEK) to form the MPL. For each measurement, a 4 μL ultrapure water droplet was made by placing the tip of the syringe close to the sample surface. The water droplet was then attached to the surface of the sample and we immediately measured the contact angle.

In order to study the influence of fluorination on FAS content, XC-72R-HNO₃ was fluorinated by different FAS contents (5, 10, 20 and 30 vol%) and the surface contact angle was measured as indicated above.

Additionally, surface morphology of cathodic MPLs fabricated from XC-72R and F-XC-72R was characterized by scanning electron microscopy (SEM, JSM-6700F).

2.2 Preparation of MEA

The membrane pretreatment procedures involved boiling the membrane in 5 vol% H₂O₂ solution, washing with ultrapure water, boiling in 0.5 M H₂SO₄ solution, and then washing with ultrapure water, at 80 °C for 2 h in turn. The pretreated membranes were kept in ultrapure water prior to the fabrication of MEAs.

For the anode, a slurry that consisted of multi-walled carbon nanotubes (MWCNTs) and PTFE (weight ratio 4:1) was spread onto carbon paper (TGP-H-060, 0 wt% PTFE, Toray) as the MPL and its loading was 1 mg cm⁻². Pt–Ru black (atomic ration 1:1, HiSpec 6000, Johnson Matthey) and Pt–Ru/C (Pt loading: 40%, Ru loading: 20%; HiSpec 10000, Johnson Matthey) were used as anodic catalyst in this work. Catalyst ink was prepared by mechanical stirring and sonication of a mixture containing appropriate amounts of catalyst, 5 wt% Nafion solution (DuPont), and isopropyl alcohol aqueous solution (volume ration 1:1). The ionomer content was 20%. The catalyst ink was then spread onto the MPL, with the loading of both kinds of noble metals at 3 mg cm⁻².

For the cathode, carbon materials (Vulcan XC-72R, XC-72R-HNO₃, F-XC-72R) and PTFE (weight ratio 4:1)

were spread onto carbon cloth (Type A, 20 wt% PTFE, E-TEK) for the outer MPL. Ketjen Black EC 600J (KB) was then spread onto the outer MPL as the inner MPL. Pt black (HiSpec 1000, Johnson Matthey) and Pt/C (Pt loading: 60%, HiSpec 9100, Johnson Matthey) were used as cathode catalysts. The ionomer content was 15% and both loadings were 3.0 mg cm⁻².

The anode, the Nafion 117 membrane, and cathode were sandwiched by hot-pressing at 130 °C under 6 MPa for 3 min to form an MEA.

2.3 Single cell test

The performance of the MEA was evaluated in a single cell with an active cross-sectional area of 2 × 2 cm². The MEA was sandwiched between two Au-deposited Ti plates with open areas of ca. 33% for both anode and cathode. The polarization curves of the passive μDMFCs at room temperature were obtained on an Arbin FCT testing system (Arbin Instrument Inc. USA) by using 3 M methanol aqueous solution as fuel. For each discharging current point along the polarization curve, a 2 min interval was used to obtain a stable voltage. Short-term discharging curves at different constant currents were obtained for the passive μDMFCs operating with 7.0 g of 3 M methanol aqueous solution. The durability of the MEA with F-XC-72R as the cathodic MPL material was evaluated in a single cell at a constant current density of 40 mA cm⁻² for 250 h.

2.4 Water crossover experiment

The experiment dealing with the amount of water-crossover was conducted at different constant-current discharging levels, fueled with 7.0 g of 3 M methanol aqueous solution. At the end of the discharge, the weight and concentration of the methanol aqueous solution at the anode were measured, and the initial ($m_{H_2O,i}$) and the final ($m_{H_2O,f}$) water masses at a given time of t was calculated accordingly.

In this work, the water transport coefficient (α) was used to evaluate water crossover ability, as suggested by Song [22]. α can be calculated using the following equation:

$$\frac{m_{H_2O,i} - m_{H_2O,f}}{M_{H_2O}} = \alpha \frac{IAt}{F} + \frac{IAt}{6F} \quad (1)$$

where I, A, t and F are current density, active area of the MEA, time of the measurement, and Faraday constant, respectively. The first and the second term in the right side of Eq. 1 correspond to the net water crossover, which is the combined result of electro-osmotic drag, diffusion and hydraulic permeation through the membrane, and the water consumption by electrochemical oxidation of methanol for a given time of t, respectively.

2.5 Electrochemical measurements

Electrochemical impedance spectra (EIS) were recorded using a Solartron SI2610 controlled by a PC and coupled with a potentiostat/galvanostat (EG&G Model 273A). A.C. impedance spectra were obtained at frequencies between 100 kHz and 0.01 Hz; the amplitude of the sinusoidal voltage signal did not exceed 10 mV. The final impedance was analyzed based on electrical circuit element model. The parameters were determined by regression fitting the experimental data with Z_{Simp}Win software.

For all the electrochemical measurements, the cells were placed in a thermostated container at a temperature of 25 ± 1 °C.

3 Results and discussions

3.1 IR spectra of different carbon materials

We used IR spectroscopy to study the influence of fluorination on Vulcan XC-72R. Figure 1 shows the IR spectra of XC-72R, XC-72R-HNO₃, and F-XC-72R. The IR spectra of XC-72R have strong absorbance bands around 3445 and 1630 cm⁻¹, corresponding to O–H stretching and bending vibrations, respectively; the –OH derives from absorbed water. The IR spectrum of XC-72R-HNO₃ shows bands at approximately 1728 and 1253 cm⁻¹, which are attributed to C=O and C–O stretching vibrations, respectively; suggesting that carboxylic groups have been produced on the surface of XC-72R upon oxidation. In the IR spectrum of F-XC-72R, new absorbance bands at ca. 1207 and 1151 cm⁻¹ are observed, which are attributable to C–Fx absorptions [23, 24], suggesting that the FAS is successfully introduced into XC-72R.

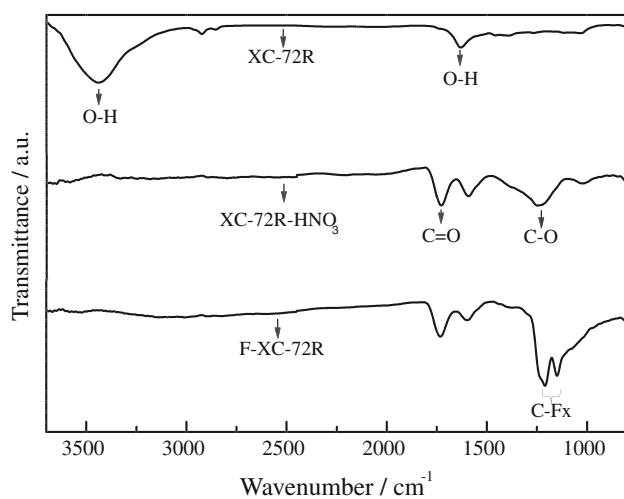


Fig. 1 FT-IR spectra of XC-72R, XC-72R-HNO₃ and F-XC-72R

3.2 Hydrophobic property of c-MPLs with different carbon materials

Figure 2 compares the contact angle for GDLs with different carbon materials on carbon cloth containing 20% PTFE. As indicated in Fig. 2A, a contact angle of 141.86° occurs when XC-72R is used as the carbon material in the MPL. After the carbon material was oxidized with HNO_3 , as confirmed by IR spectra, alcoholic and carboxylic groups are produced on the surface of XC-72R. As a result, the XC-72R- HNO_3 is more hydrophilic, and the measured contact angle becomes smaller (Fig. 2B): specifically, it is 132.46°. When XC-72R- HNO_3 was fluorinated by FAS (20 vol%), the surface of XC-72R was modified with fluorine.

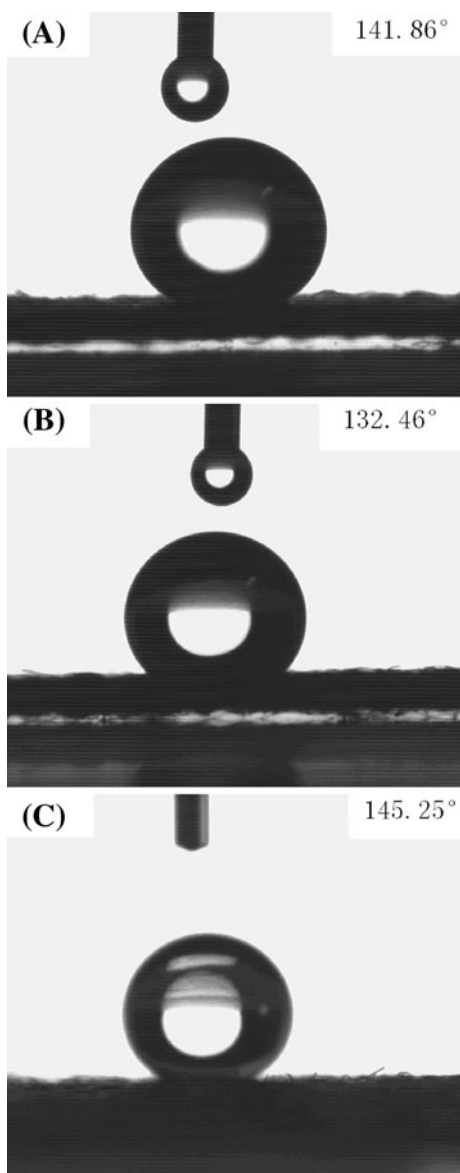


Fig. 2 Contact angle images for MPLs with different carbon materials. (A) XC-72R, (B) XC-72R- HNO_3 and (C) F-XC-72R

As is well known, fluorine is effective for lowering the surface free energy because of its small atomic radius, and having the greatest electronegativity among all atoms. As a result, FAS forms a stable covalent bond with carbon. Figure 2C indicates that the modified material has the greatest contact angle of 145.25°. As mentioned earlier, the cathodic MPL carbon material was treated to make it more hydrophobic in order to optimize oxygen transport and water management.

Additionally, contact angle measurement of fluorinated XC-72R- HNO_3 with various FAS contents was conducted. Figure 3 shows the relationship between FAS content and the contact angle on the surface of the MPL. With increasing FAS content, the contact angle increases slightly.

3.3 Morphological characteristics of the cathodic MPLs

Figure 4 presents the SEM micrographs of cathodic MPL with XC-72R and F-XC-72R, respectively. As it can be seen from Fig. 4, both samples are porous, due to the accumulated carbon particles. However, the microstructures of F-XC-72R are different from that of XC-72R. The MPL with XC-72R has larger pores than that with F-XC-72R, while the MPL with F-XC-72R exhibits more compact pore structure. Such the compact pore structure may be beneficial to the oxygen mass transfer and water back diffusion. In addition, the compact and uniform microstructure also reduces the catalyst loss through the GDL during the fabrication process, thus leading to a slight improvement in catalyst utilization of the cathode. Such a hypothesis was verified by calculating the H adsorption/desorption areas in cyclic voltammograms.

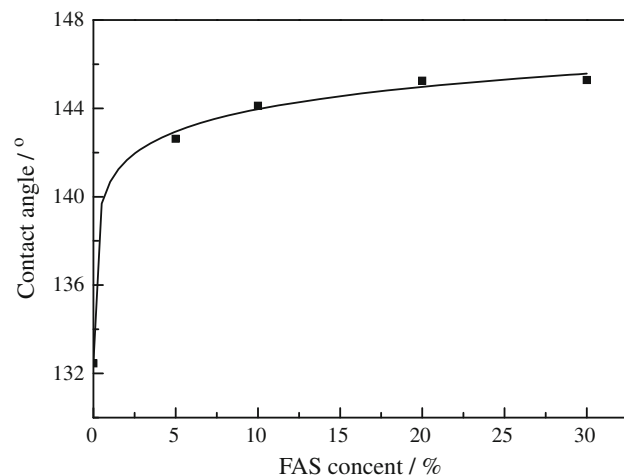


Fig. 3 Relationship between FAS content and the contact angle on MPL

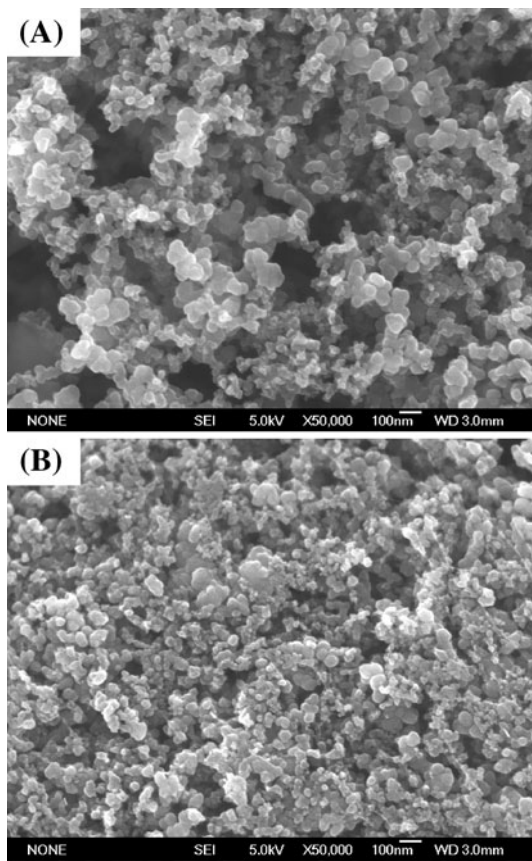


Fig. 4 SEM micrographs of the MPLs with (A) XC-72R and (B) F-XC-72R

3.4 Performance comparison of passive μ DMFCs

Figure 5 is a performance comparison of five passive μ DMFCs using different carbon materials and various carbon loadings within cathodic MPLs. From Fig. 5, one can find that the performance of the cell using XC-72R-HNO₃, at higher current densities, is not as good as that of XC-72R; but passive DMFCs with fluorinated XC-72R as the outer cathodic MPL perform significantly better than that using XC-72R. Moreover, the performance of passive μ DMFCs varies with the loading of fluorinated XC-72R. In the low current density region, the five μ DMFCs exhibited similar kinetic and ohmic polarization behaviors, which is reasonable since the same anode and cathode catalysts were used for five μ DMFCs. However, as the current density increases, the polarization curves with fluorinated XC-72R show a smaller voltage drop compared with that of XC-72R and XC-72R-HNO₃, demonstrating that fluorination of XC-72R has a significant influence on the mass transport of a μ DMFC. A reasonable supposition is that fluorination of XC-72R changes the surface hydrophobicity of XC-72R, which builds up a high liquid pressure that drives water flow back to the anode and improves oxygen

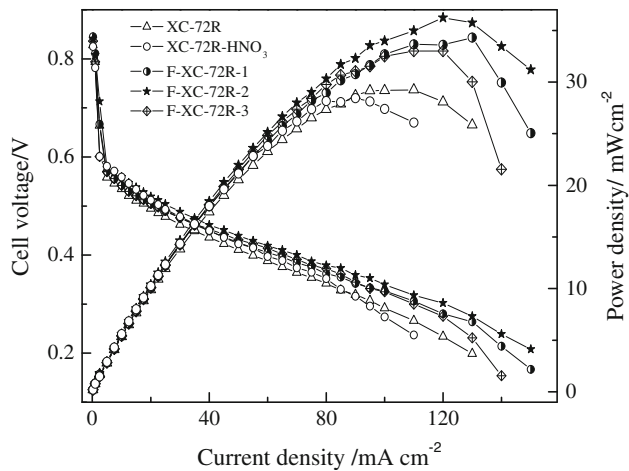


Fig. 5 Polarization curves of passive μ DMFCs with different carbon materials and various loadings within the cathodic MPL

transport to the cathode side, especially when operating under high current densities. For fluorinated XC-72R as the outer cathodic MPL and a loading of 2 mg cm⁻², the maximal power density is found to be ca. 36.2 mW cm⁻². On the other hand, when the loadings of F-XC-72R are 1 and 3 mg cm⁻², the maximal power densities of the cells are about 34.3 and 33.0 mW cm⁻², respectively. The performance is improved comparing to the references, i.e., the maximal power densities of the cells using XC-72R and XC-72R-HNO₃ are only 29.3 and 28.4 mW cm⁻², respectively.

3.5 Stability comparison of passive μ DMFCs

The MEA performance with fluorinated XC-72R as the outer cathodic MPL material is substantially higher than that of MEA with XC-72R. For practical application, it is important to investigate the stability in addition to the short term performance. Figure 6A exhibits a 3 h discharging test of two passive DMFCs with 2 mg cm⁻² of XC-72R and F-XC-72R within the outer cathodic MPLs at a constant current density of 40 mA cm⁻². In Fig. 6B, the voltages of two curves have been normalized, where V₀ is the initial voltage during discharging. Obviously, the cell with F-XC-72R is shown to be more stable than that with XC-72R. After 3 h operation, the voltage of the cell with F-XC-72R decreases by 10.3%, compared with 19.8% for XC-72R. In addition, it was found after testing that water flooding in cathode with F-XC-72R is less serious. The enhanced stability of the cell with F-XC-72R is possibly attributed to its optimized mass transport: the MPL using fluorinated XC-72R has appropriate hydrophobicity and pore size distribution, which favor oxygen transfer from the air to the catalyst and also water removal.

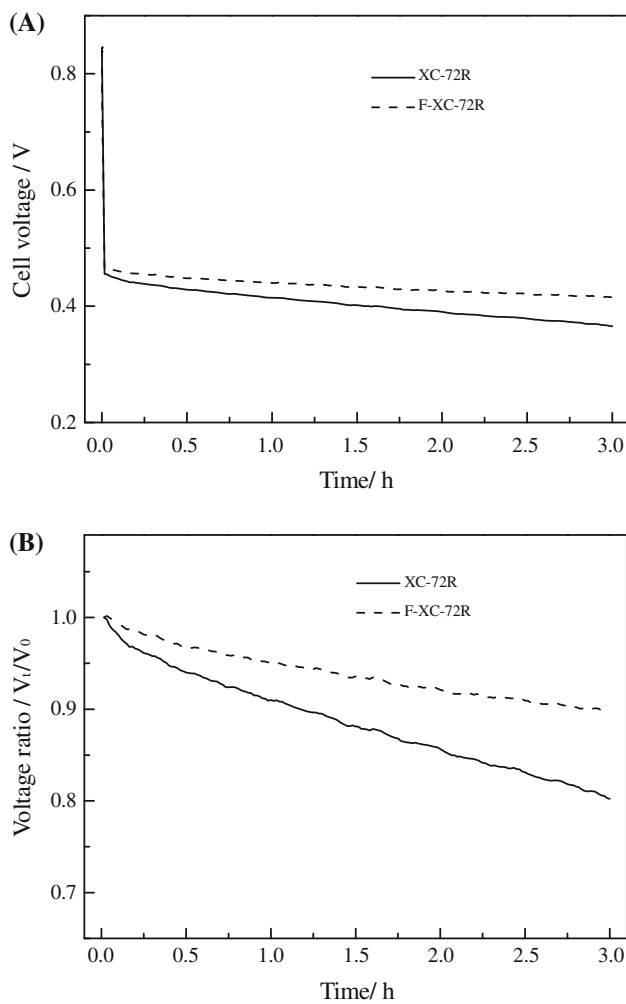


Fig. 6 Discharging curves (A) and voltage normalized curves (B) of two passive μ DMFCs with XC-72R and F-XC-72R within outer cathodic MPL at a discharging current density of 40 mA cm^{-2}

To further evaluate the enhanced durability of the passive DMFC using F-XC-72R as outer cathodic MPL material, the long-term operation at a current density of 40 mA cm^{-2} is shown in Fig. 7. It was found that the discharging voltage fluctuates in short term and trends to a steady state in long-term operation. The short-term voltage decay might be ascribed to the consumption of the methanol at anode and the water flooding at cathode. The cell voltage only shows a very slight decrease during the 250 h operation, assessing that the durability of the cell with F-XC-72R is promising for a practical application with an improved cell performance.

3.6 Influence of the outer cathodic MPL on water crossover

In order to determine the influence of outer cathodic MPL on water management, we estimated the water transport

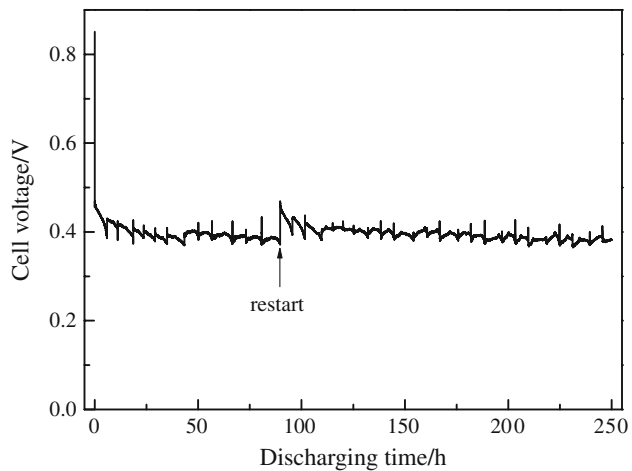


Fig. 7 Long-term durability test of a passive μ DMFC with F-XC-72R as outer cathodic MPL material at a discharging current density of 40 mA cm^{-2}

coefficient (α) using Eq. 1. As indicated in Fig. 8, for passive μ DMFCs, the increase of current density results in the decrease of α . Moreover, α value of the cell using F-XC-72R is less than that of XC-72R at all discharging current densities. We infer that higher hydrophobicity and more compact pore structure lead to smaller water transport coefficients α . On one hand the higher hydrophobicity builds up higher liquid pressure on the cathode, resulting in reverse water flow from cathode to the anode. On the other hand it also favors the removal of water from the cathodic MPL via gasification. Both mechanisms would improve water management and decrease cathodic water flooding.

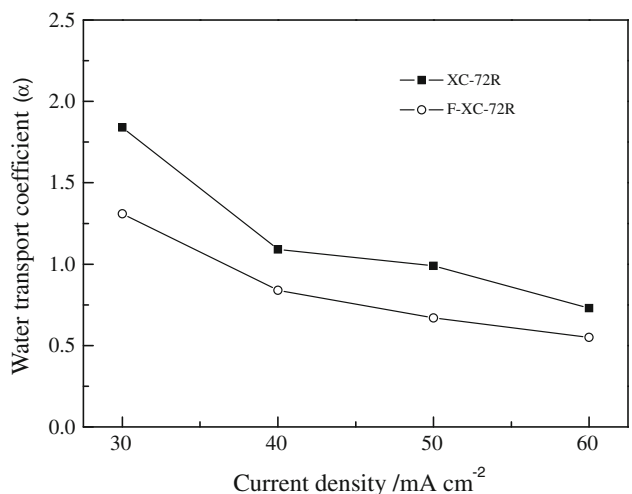


Fig. 8 The measured water transport coefficient of two passive μ DMFCs with XC-72R and F-XC-72R within outer cathodic MPLs at different current densities

3.7 EIS analyses

EIS of the MEAs in the passive μ DMFCs were analyzed to explore the impact of the outer cathodic MPL materials on cell performance. Figure 9A shows impedance spectra together with fitted curves based on an equivalent circuit model as shown in Fig. 9B. The indicated points are the experimental data, while the curves are the fits of the data to functional expressions. In the applied model, the constant phase elements (CPEs) are used to replace ideal capacitors, which are commonly used in conventional equivalent circuit models, to account for the non-uniform structure of the related electrode section [25, 26]. Two CPEs were employed in the present model in order to account for the influences of anodic and cathodic catalytic layers. The physical meanings of each element employed in the equivalent circuit model (Fig. 9B) are shown as follows:

- (1) R_1 denotes the ohmic resistance, R_2 and L_1 contributes to the resistance and inductance of the conducting cables;
- (2) The cathode contribution contains R_3 and CPE_1 , which describe the charge transfer resistance and capacitive nature of the real cathode with roughness of the catalyst layer and non-uniform catalyst distribution;
- (3) The capacitor CPE_2 describes the capacitive behavior of the real anode, which intrinsically possesses

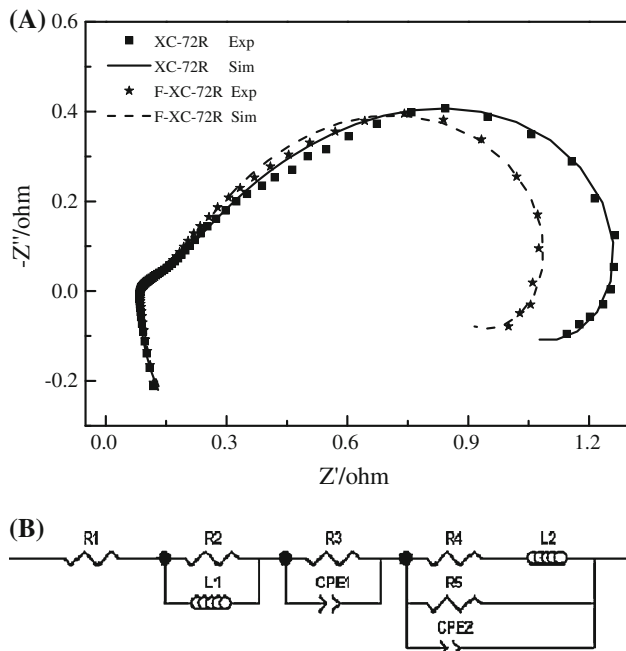


Fig. 9 (A) EIS spectra and (B) equivalent circuit of the μ DMFCs using XC-72R and F-XC-72R as outer cathodic MPL materials at a given DC potential of 0.5 V

roughness in the catalyst layer as well as a non-uniform catalyst distribution. The inductance L_2 accounts for the fact that the current is phase delayed with respect to the voltage perturbation because of the slowness of CO desorption. R_4 is used to modify the phase-delay, and R_5 is attributed to the part of the current response that occurs without change in the surface coverage, as described previously.

Figure 9A shows that the simulation, using the CPE-based model, fits the experimental data essentially over the full range of frequencies; fitted parameters are presented in Table 1. As observed, the ohmic resistance (R_1) of the cell using F-XC-72R, corresponding to the intercept in the high-frequency domain on the Z' axis, was larger than that of XC-72R; an explanation for this is that FAS is insulator material gives rise to a larger ohmic resistance of MPL, and as a result, a larger total ohmic resistance.

It is further observed that use of F-XC-72R results in a decrease of the charge transfer resistance for the oxygen reduction reaction, which is ascertained from the fitted data (parameter R_3 , Table 1). The use of F-XC-72R results in a lower charge transfer resistance (0.266 ohm cm^2) than does the use of XC-72R (0.399 ohm cm^2). Again, this results from the greater hydrophobicity and compact pore structure when F-XC-72R is used, which promotes oxygen diffusion to the cathode, leading to an enhancement in cell's performance.

4 Conclusions

This work has dealt with the fluorination of XC-72R with FAS, and improved properties of the material when used in the cathodic MPL of a passive μ DMFC. Contact angles on the surface of MPL were compared, which showed that the

Table 1 Fitted parameters for the CPE-based equivalent circuit model for two μ DMFCs using XC-72R and F-XC-72R within outer cathodic MPLs

Parameter	XC-72R	F-XC-72R
R_1 (ohm)	0.0822	0.0853
L_1 (Henri)	3.651E-7	3.500E-7
R_2 (ohm)	1.106	1.095
R_3 (ohm)	0.398	0.266
CPE_1 (F)	0.499	0.385
n_1	0.801	0.692
R_4 (ohm)	1.802	1.522
L_2 (H)	16.4	13.6
R_5 (ohm)	1.55	1.559
CPE_2 (F)	0.989	1.164
n_2	0.801	0.657

MPL becomes more hydrophobic when F-XC-72R is used. High hydrophobicity of the cathodic MPL promotes oxygen mass-transport and reduces cathodic water flooding. Upon optimization of the outer cathodic MPL structure with fluorinated XC-72R, the cell performance improved substantially. We also found that the calculated water transport coefficient decreased, which confirms that more water in the cathode flows backwards to the anode. Also, impedance analysis indicated that the improved performance of the passive μ DMFC with fluorinated XC-72R can be attributed to the decreased charge transfer resistance of the cathodic reaction.

Acknowledgments We would like to thank the National Natural Science Foundation of China (20706056), the National “863” High-Tech Research Programs of China (2006AA05Z136, 2007AA05Z141, 2008AA05Z102), and the 100 People Plan Program and the Knowledge Innovation Engineering of the CAS for support of this work. Also, DLA thanks the National Science Foundation of the USA for support under Cooperative Agreement HRD-0833180.

References

1. Yang WW, Zhao TS (2007) *Electrochim Acta* 52(20):6125
2. Kim H, Oh J, Kim J et al (2006) *J Power Sources* 162(1):497
3. Zhao TS, Chen R, Yang WW et al (2009) *J Power Sources* 191(2):185
4. Chan YH, Zhao TS, Chen R et al (2008) *J Power Sources* 176(1):183
5. Li J, Ye D, Zhu X et al (2009) *J Appl Electrochem* 39(10):1771
6. Zhao TS, Xu C, Chen R et al (2009) *Prog Energy Combust Sci* 35(3):275
7. Liu H, Song C, Zhang L et al (2006) *J Power Sources* 155(2):95
8. Mao Q, Sun GQ, Wang S et al (2008) *J Power Sources* 175(2):826
9. Lin GY, Van Nguyen T (2005) *J Electrochem Soc* 152(10):A1942
10. Weber AZ, Newman J (2005) *J Electrochem Soc* 152(4):A677
11. Qi Z, Kaufman A (2002) *J Power Sources* 109(1):38
12. Pasaogullari U, Wang CY (2004) *Electrochim Acta* 49(25):4359
13. Wang XL, Zhang HM, Zhang JL et al (2006) *Electrochim Acta* 51(23):4909
14. Passalacqua E, Squadrito G, Lufrano F et al (2001) *J Appl Electrochem* 31(4):449
15. Park S, Lee JW, Popov BN (2006) *J Power Sources* 163(1):357
16. Park GG, Sohn YJ, Yang TH et al (2004) *J Power Sources* 131(1–2):182
17. Kong CS, Kim DY, Lee HK et al (2002) *J Power Sources* 108(1–2):185
18. Wang T, Lin C, Fang Y et al (2008) *Electrochim Acta* 54(2):781
19. Liu F, Lu G, Wang C (2006) *J Electrochem Soc* 153(3):A543
20. Xu C, Zhao TS, He YL (2007) *J Power Sources* 171(2):268
21. Krishnamurthy B, Deepalochani S (2009) *Int J Hydrogen Energy* 34(1):446
22. Song KY, Lee HK, Kim HT (2007) *Electrochim Acta* 53(2):637
23. Nishino T, Urushihara Y, Meguro M et al (2004) *J Colloid Interface Sci* 279(2):364
24. Kharitonova AP, Moskvina YL, Teplyakov VV et al (1999) *J Fluorine Chem* 93(9):129
25. Reshetenko TV, Kim HT, Kweon HJ (2008) *Electrochim Acta* 53(7):3043
26. Mueller JT, Urban PM (1998) *J Power Sources* 75(1):139